


Identification of key genes and pathways in IgA nephropathy using bioinformatics analysis

Shou-Liang Hu, MM^a, Dan Wang, MM^b, Fan-Li Yuan, MM^a, Qing-Feng Lei, MM^a, Yong Zhang, MM^c, Jun-Zhang Cheng, MM^{a,*}

Abstract

Background: IgA nephropathy (IgAN) is the most frequent type of primary glomerulonephritis globally and the leading cause of end-stage renal disease in young adults. Its pathogenesis is not fully known, but is largely attributed to genetic factors. This study was aimed to explore the prognostic values of key genes in IgAN.

Methods: The gene expression profile GSE93798 of 20 IgAN samples and 22 normal samples using glomeruli from kidney biopsy was adopted. Totally 447 upregulated and 719 downregulated differentially expressed genes were found in IgAN patients on the R software. The Gene Ontology enrichment and the Kyoto Encyclopedia of Gene and Genomes pathway were investigated on DAVID, and the protein-protein interaction network and the top 13 hub genes of the differentially expressed genes were built via the plug-in molecular complex detection and cytoHubba of Cytoscape.

Results: From the protein-protein interaction network, of the top 13 hub genes, FOS, EGFR, SIRT1, ALB, TFRC, JUN, IGF1, HIF1A, and SOCS3 were upregulated, while CTTN, ACTR2, CREB1, and CTNBN1 were downregulated. The upregulated genes took part in the HIF-1 signaling pathway, Choline metabolism in cancer, Pathways in cancer, Amphetamine addiction, Estrogen, TNF, and FoxO signaling pathways, and Osteoclast differentiation, while the downregulated genes were involved in Pathogenic *Escherichia coli* infection, Bacterial invasion of epithelial cells, prostate cancer, and melanogenesis.

Conclusion: This study based on the Gene Expression Omnibus database updates the knowledge about the mechanism of IgAN and may offer new treatment targets.

Abbreviations: DEGs = differentially expressed genes, ECM = extracellular matrix, IgAN = IgA nephropathy, KEGG = Kyoto Encyclopedia of Genes and Genomes, MCODE = molecular complex detection, PPI = protein-protein interaction, PTC = peritubular capillary.

Keywords: bioinformatics, IgA nephropathy, key genes, pathways

1. Introduction

Immunoglobulin A nephropathy (IgAN) identified by Jacques Berger 50 years ago^[1] was once considered as an uncommon variant of mesangial proliferative glomerular disease, but was actually the leading primary glomerulonephritis worldwide.^[2,3] The International Kidney Biopsy Survey on glomerular disease

frequency involving over 42,000 renal biopsies in 4 continents showed IgAN was identified in 22% and 39% of all glomerular diseases in Europe and Asia respectively.^[4] Despite its generally benign course in clinic, finally 15% to 20% of the patients within 10 years and 30% to 40% within 20 to 30 years after the first onset will develop to end-stage renal disease.^[5]

IgAN is a complex disease with variable clinical and pathological features, but its exact pathogenesis is only partially known. The causes and development of IgAN are ascribed to genetic factors given its varying incidence among ethnicities and its high familial aggregation. Multiple genes and signaling pathways have been suggested to take part in the initiation and development of IgAN. Thus, studying the molecular mechanism or pathology of IgAN is extremely important in order to find out more efficient diagnostic, therapeutic, and prognostic methods. So far, the microarray technique plus bioinformatics has facilitated the analysis of DNA or RNA expression changes amid the variation and prognosis of IgAN. We can also explore the interactions among differentially-expressed genes (DEGs) and study the enrichment pathways and functional annotation and in the interaction network.

In this study based on bioinformatics, we investigated DEGs, the enrichment of GO terms or pathways, and protein-protein interaction (PPI) in IgAN by using the samples of GSE93798 in order to predict potential targets. We also analyzed the modules and their functions in each PPI network and sought to determine possible hub genes using cytoHubba and a network analyzer. Finally, the common genes of the 5 methods were selected as the hub genes.

Editor: Undurti N. Das.

S-LH and DW contributed equally to this study.

The authors report no conflicts of interest.

The datasets generated during and/or analyzed during the current study are publicly available.

^a Division of Nephrology, ^b Central Laboratory, The First Hospital of Yangtze University, ^c Division of Nephrology, Jianli County People's Hospital, Hubei, Jingzhou, China.

* Correspondence: Jun-Zhang Cheng, Division of Nephrology, The First Hospital of Yangtze University, Hubei, Jingzhou, China (e-mail: cjz_1954@126.com).

Copyright © 2020 the Author(s). Published by Wolters Kluwer Health, Inc. This is an open access article distributed under the terms of the Creative Commons Attribution-Non Commercial License 4.0 (CCBY-NC), where it is permissible to download, share, remix, transform, and buildup the work provided it is properly cited. The work cannot be used commercially without permission from the journal.

How to cite this article: Hu SL, Wang D, Yuan FL, Lei QF, Zhang Y, Cheng JZ. Identification of key genes and pathways in IgA nephropathy using bioinformatics analysis. *Medicine* 2020;99:30(e21372).

Received: 4 January 2020 / Received in final form: 11 June 2020 / Accepted: 18 June 2020

<http://dx.doi.org/10.1097/MD.00000000000021372>

2. Materials and methods

2.1. Microarray data

The Gene Expression Omnibus (free on www.ncbi.nlm.nih.gov/geo) provides original submitter-offered records and curated datasets. The microarray profile dataset GSE93798 in IgAN (including 20 IgAN kidney biopsy samples and 22 normal samples) was obtained from the Affymetrix GPL22945 platform (Affymetrix Human Genome U133 Plus 2.0 Array), which was uploaded by Liu et al in January 18, 2017 and updated in October 13, 2017. Data were pretreated and DEGs were identified using the Bioconductor in R software and the original data were preprocessed using the Affy package. Firstly, the raw data of intensity were treated by background calibration, log₂ transformation, and quantile normalization. Then the potential batch impacts of the pooled datasets were detected via the principal component analysis. Finally, the normalized data were fitted by a linear model to form an expression measure set on the qualified dataset. The DEGs for each disease were chosen using the empirical Bayes method and the significant DEGs were set at $P < .05$ after adjustment by the Benjamini–Hochberg method. Fold change of the expression of individual gene was also observed for differential expression test. The DEGs with false discovery rate (FDR) < 0.05 and $|\log \text{fold change}| > 1.5$ were considered to be significant.

2.2. GO and Kyoto Encyclopedia of Genes and Genomes (KEGG) pathway enrichment analysis

The GO enrichment and KEGG pathway of DEGs were analyzed at the function level on DAVID 6.7 (david.ncifcrf.gov), which offers a complete set of gene function annotation tools. $P < .05$ was regarded as significant difference.

2.3. PPI network analysis

The functional interactions among these DEGs were further explored using a PPI network. The DEGs were plotted via the tool

STRING (www.string-db.org) and the interactions validated at a combined score of > 0.5 were chosen. Then the PPI network was built and visualized on Cytoscape 3.4.0 and the modules of the network were identified using the plug-in Molecular Complex Detection (MCODE) as per the criteria of MCODE score ≥ 4 and node number > 4 . The function enrichment of DEGs in the top module was analyzed with DAVID.

2.4. Identification of hub genes

To balance between the core genes and avoid the missing of the key gene, we extracted the hub genes using cytoHubba and through the cytoHubba plugin, obtained 12 topological analysis methods. The top 25 hub-forming genes/proteins were identified based on MCC, MNC, degree, closeness, and betweenness separately. Then the overlapping genes were chosen as the hub genes. Finally, the common genes were found using Venn diagrams (<http://bioinformatics.psb.ugent.be/webtools/Venn/>).

2.5. Ethical statement

All the data of this paper was obtained from the open-access database, we did not get these data from patients or animals directly, nor intervene these patients. So the ethical approval was not necessary.

3. Results

3.1. The DEGs

A total of 1166 DEGs were finally screened out from the IgAN samples and compared with the normal samples, including 447 upregulated and 719 downregulated DEGs. The heat map of the DEGs and the volcano plot are displayed in Figure 1A and B, respectively.

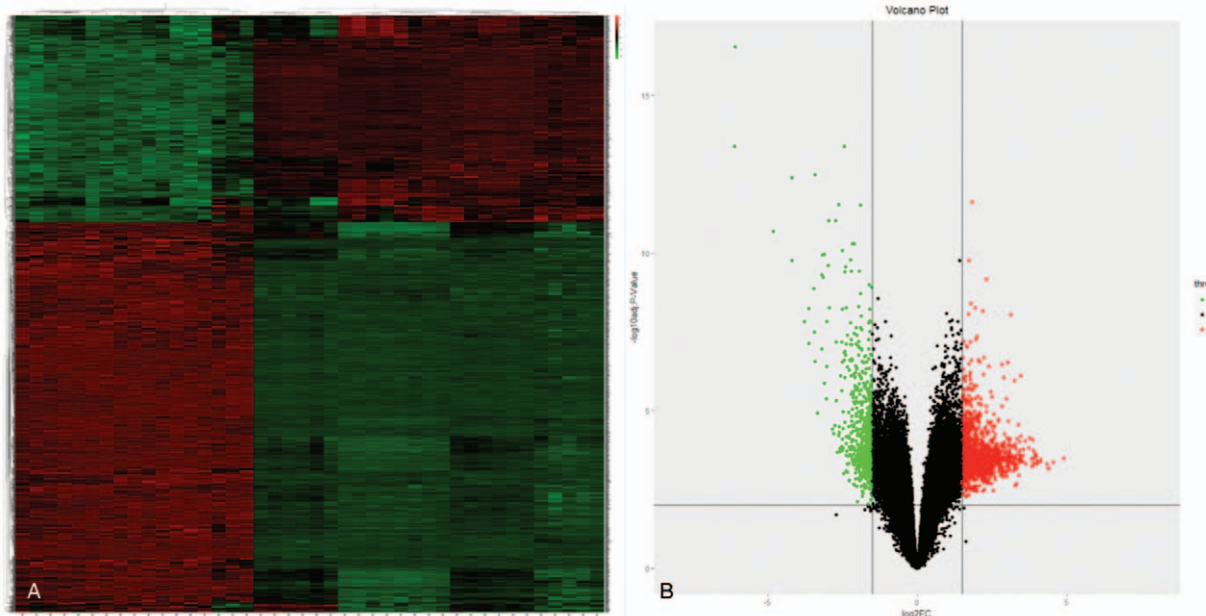


Figure 1. (A) Heatmap and (B) volcano plot for DEGs. DEGs = differentially expressed genes.

Table 1**GO analysis of upregulated and downregulated differentially expressed genes in biological processes.**

A, Upregulated			
Term	Function	Count	P-value
GO:0048661	Positive regulation of smooth muscle cell proliferation	8	5.22×10^{-4}
GO:0042493	Response to drug	18	9.84×10^{-4}
GO:0035914	Skeletal muscle cell differentiation	7	.001008892
GO:0045444	Fat cell differentiation	8	.001692924
GO:0006805	Xenobiotic metabolic process	8	.002482084
B, Downregulated			
Term	Function	Count	P-value
GO:0098609	Cell-cell adhesion	33	2.42×10^{-8}
GO:0048010	Vascular endothelial growth factor receptor signaling pathway	14	3.65×10^{-6}
GO:0030036	Actin cytoskeleton organization	18	1.22×10^{-5}
GO:0018105	Peptidyl-serine phosphorylation	17	2.86×10^{-5}
GO:1903608	Protein localization to cytoplasmic stress granule	5	7.31×10^{-5}

GO = gene ontology.

3.2. Go term enrichment

The DEGs were imported to the DAVID for GO and KEGG pathway analysis. As for the bioprocesses, the upregulated DEGs were considerably enriched in positive modulation of smooth muscle cell growth, drug reaction, skeletal muscle cell division, fat cell division, and xenobiotic metabolism, while the downregulated DEGs were concentrated in cell-cell adhering, vascular endothelial growth factor receptor pathway, actin cytoskeleton

organization, peptidyl-serine phosphorylation and protein localization to cytoplasmic stress granule (Table 1).

3.3. KEGG pathway analysis

The KEGG pathways of the DEGs were analyzed using DAVID (Table 2). The upregulated DEGs were mainly involved in tyrosine metabolism, drug metabolism-cytochrome P450, Valine, leucine and isoleucine degradation, and prostate cancer and

Table 2**KEGG pathway analysis of upregulated and downregulated differentially expressed genes. Top 5 terms were selected according to P-value when more than 5 terms enriched terms were identified in each category.**

A, Upregulated				
Pathway ID	Name	Count	P-value	Genes
hsa00350	Tyrosine metabolism	5	.012844	AOX1, ADH5, ADH6, HGD, MIF
hsa00982	Drug metabolism- cytochrome P450	6	.032779	FM01, AOX1, ADH5, ADH6, UGT2B28, MGS1
hsa00280	Valine, leucine and isoleucine degradation	5	.034349	BCKDHA, MCCC2, ACADSB, AOX1, ABAT
hsa05215	Prostate cancer	6	.081613	FGFR2, EGFR, IGF1, PDGFC, TCF7L2, CHUK
hsa00830	Retinol metabolism	5	.087275	RDH10, AOX1, ADH5, ADH6, UGT2B28
B, Downregulated				
Pathway ID	Name	Count	P-value	Genes
hsa04810	Regulation of actin cytoskeleton	31	2.61×10^{-8}	GNA13, PDGFA, WASF2, ABI2, RDX, GNG12, ITGB3, ARPC5, ITGB1, PFN1, EZR, PAK2, ITGB8, RAC1, SOS2, RHOA, BRK1, FGF1, PIK3R3, APC, FN1, VAV3, BRAF, PIK3CB, MYLK3, ITGA1, MYL12A, ARHGEF12, NCKAP1, CFL1, CRK
hsa04722	Neurotrophin signaling pathway	20	2.17×10^{-6}	BRAF, PIK3CB, YWHAE, PDPK1, PSEN1, GSK3B, GAB1, NTRK2, SOS2, RAC1, RHOA, CALM3, SORT1, SHC1, PIK3R3, MAP2K7, CRK, ARHGDI, AKT3, AKT2
hsa04510	Focal adhesion	27	2.64×10^{-6}	TLN1, PDGFA, ITGB3, ITGB1, CTNNA1, PDPK1, PAK2, ITGB8, SOS2, RAC1, RHOA, SHC1, PIK3R3, AKT3, FN1, AKT2, VAV3, BRAF, PIK3CB, MYLK3, ITGA1, MYL12A, COL5A2, CCND2, GSK3B, VEGFA, CRK
hsa05200	Pathways in cancer	39	1.03×10^{-5}	GNA13, HSP90AB1, PDGFA, GNA11, BCL2L1, GNG12, ITGB1, CTNNA1, AGTR1, MAX, RAC1, SOS2, RHOA, TPR, PIK3R3, FGF1, AKT3, APC, AKT2, FN1, EPAS1, BRAF, PIK3CB, RXRB, TGFB2, CDK6, RB1, ARHGEF12, CTNNA1, FZD4, STK4, DAPK1,
hsa04611	Platelet activation	19	2.72×10^{-5}	GNA13, TLN1, PIK3CB, MYLK3, PRKCI, MYL12A, ITGB3, ARHGEF12, ITGB1, COL5A2, ITPR1, P2RY1, RHOA, FCER1G, FCGR2A, SNAP23, PIK3R3, AKT3, AKT2

KEGG = Kyoto Encyclopedia of Genes and Genomes.

Table 3
Five modules from the protein-protein interaction network satisfied the criteria of MCODE scores ≥ 4 and number of nodes > 4 .

Cluster	Score	Nodes	Edges	Node IDs
1	14.772	58	421	UBA6, CSTF2T, SSR1, RNF144B, SSR3, TFRC, RNF4, AGTR1, YBX1, FBXO30, VAMP2, HUWE1, SGIP1, SH3GL2, FBXO9, ITC, SYT2, STAM2, FCHO2, CUL3, UBE2H, FBXL20, RPL14, SEC61B, DNAJC6, RPS27L, TRAM1, SRP68, SRP72, DDX42, GAK, AAK1, DHX9, CPSF2, SNRPE, SNRPB, RNF6, SCARB2, KLHL5, HECTD1, RPL27A, RAB5C, RPL31, SF3B4, CDC5L, EGFR, DDX46, RPL37A, FBXW11, DNAJC8, SRRM2, RPL38, FZD4, ARPC5, PRPF40A, RPLP2, SOCS3, UFL1
2	11.222	37	202	TAOK1, PRKAR2B, JUN, PCM1, HAUS3, HAUS6, AKT2, DYNC1L1, CREB1, STAG2, TCTN2, CC2D2A, SIRT1, EIF3M, ALB, CTNNB1, SDHC, AKT3, EIF4E, ACTR1A, RANBP2, SMC3, MDM2, YWHA, EIF2S3, BUB3, SKA2, NSL1, SMC1A, HSPA4, IGF1, FOS, CEP76, BCL2L1, EGR1, HIF1A, VEGFA
3	7	7	21	VAV3, FCGR2A, BAIAP2, NCKAP1, WASF2, ABI2, BRK1
4	6.286	36	110	RB1, MRPS15, NTRK2, SOD2, RPRD1A, GSPT1, HBEGF, DNAJB4, P4HB, GTF2A1, HSPA14, CDK9, GFM1, DNAJA2, FSTL1, SNAPC3, TAF6, SUPT4H1, FGFR2, DNAJC3, SDC2, GSK3B, BTG2, SHC1, ELL2, SERPINA1, SUGT1, DUSP1, TAF13, FGA, RHOA, CENK, GRPEL2, IGFBP1, HSPH1, VCAN
5	4.8	36	84	HIST3H2A, DNAH9, HIST1H4H, ATP6AP2, DNALI1, TPR, SNAP23, DYNC1I2, KAT2B, B4GALT1, CD274, HIST1H4E, DNAJC13, FCER1G, CYBA, LILRB2, RAP2C, WDR60, PDGFA, PDGFC, TAF9B, NQO1, SUPT6H, MGST1, FGF1, ATP11B, PCGF2, LAMP2, TADA2B, MYSM1, KDM4B, CMTM6, ING4, PSMC2, USP22, EEF1D

MCODE=molecular complex detection, Score=(density \times no. of nodes).

retinol metabolism. The downregulated DEGs were mainly involved in actin cytoskeleton, neurotrophin pathway, focal adhesion, pathways in cancer and platelet activation.

3.4. PPI network construction and module analysis

A total of 5 modules from the PPI network were identified with MCODE score ≥ 4 and node number > 4 (Table 3) and the top 3 modules were chosen (Fig. 2). As for KEGG pathway enrichment, the 3 modules were mainly involved in modulating actin cytoskeleton, HTLV-I infection, cancer pathways, PI3K-Akt pathway, and HIF-1 pathway.

3.5. Hub gene selection

The hub genes were screened out by overlapping the genes according to 5 ranked methods in cytoHubba (Fig. 3A). Thirteen hub genes were selected, including 9 with upregulation and 4 with downregulation. The details are shown in Table 4 and visualized in Figure 3B. Results show the functions of the 13 hub genes and their probable role in IgAN, indicating they may be novel therapeutic target genes.

4. Discussion

With the 20 IgAN samples and 22 normal samples from GSE93798, totally 447 upregulated genes and 719 downregulated genes were found. As for GO enrichment, the upregulated DEGs were considerably concentrated in positively regulating smooth muscle cell proliferation, response to drug, skeletal muscle cell division, fat cell division, and xenobiotic metabolism, and the downregulated DEGs were mainly involved in cell-cell adhesion, vascular endothelial growth factor (VEGF) receptor pathway, actin cytoskeleton organization, peptidyl-serine phosphorylation and protein positioning to cytoplasmic stress granule. Furthermore, the KEGG pathways were tyrosine metabolism, drug metabolism-cytochrome P450, Valine, leucine and isoleucine degradation, prostate cancer, and retinol metabolism for the upregulated DEGs, while were actin cytoskeleton, neurotrophin pathway, focal adhesion, pathways in cancer and platelet activation for the downregulated DEGs. Among these DEGs, 13 hub genes were selected in the PPI

network by cytoHubba, including FOS, EGFR, SIRT1, ALB, TFRC, JUN, IGF1, HIF1A, SOCS3, ACTR2, CREB1, CTNNB1, and CTTN. The first 9 genes were upregulated and the latter 4 were downregulated in IgAN patients.

Among the FOS family (including FOS, FOSB, FOSL1, and FOSL2), FOS is involved in the molecular mechanisms of cell growth, division, apoptosis, and migration.^[6] Some proto-oncogenes were overexpressed glomerularly in IgAN patients.^[7-9] FOSL1 may promote the progression of podocyte foot affacement in IgAN to induce glomerular injury, suggesting FOSL1 may be associated with IgAN severity.^[10] FOS is connected with DNA destruction, telomere injury-caused aging markers, and neutrophil actions, which regulate the initiation and evolution of IgAN.^[11]

Growth hormone and insulin-like growth factor IGF(-1) can considerably affect the kidney growth, actions and structural conservation and are associated with extracellular matrix (ECM) reshaping, and podocyte and mesangial cell growth.^[12] These findings indicate the role of IGF-1 in the pathogenesis of IgAN. IGF-1 can be generated and released by mesangial cells and activate downstream signaling molecules (eg, phosphatidylinositol 3 [PI3] kinase and extracellular signal-regulated protein kinase [ERKs]). These activities are seemingly related with the renewing and components of glomerular ECM, leading to the occurrence of kidney diseases.^[13-15] IGF-1 is largely associated with pathology,^[16] and the altered IGF-1/1R function may affect the development of glomerular sclerosis or interstitial fibrosis. The rs1520220 and rs2195239 variants were related with the pathologic grades in IgAN patients, but neither was found significantly related with the susceptibility to IgAN in all genetic models.^[17]

Hypoxia is one of the key causes of kidney damage. Though acutely-impaired kidneys may benefit from the positive effects of HIF-modulated bioprocesses,^[18-20] partial HIF-1 α -mediated chronic hypoxia can intensify ECM production and epithelial-mesenchymal transition, which may facilitate renal fibrosis and kidney diseases.^[21-23] Among various kidney diseases, progressive interstitial fibrosis is related to peritubular capillary (PTC) loss around the renal tubules and consequently renal dysfunction.^[24] PTC loss in chronic tubulointerstitial damage is also connected with the expression alteration of VEGF, an inductor that regulates capillary growth and vessel formation in several

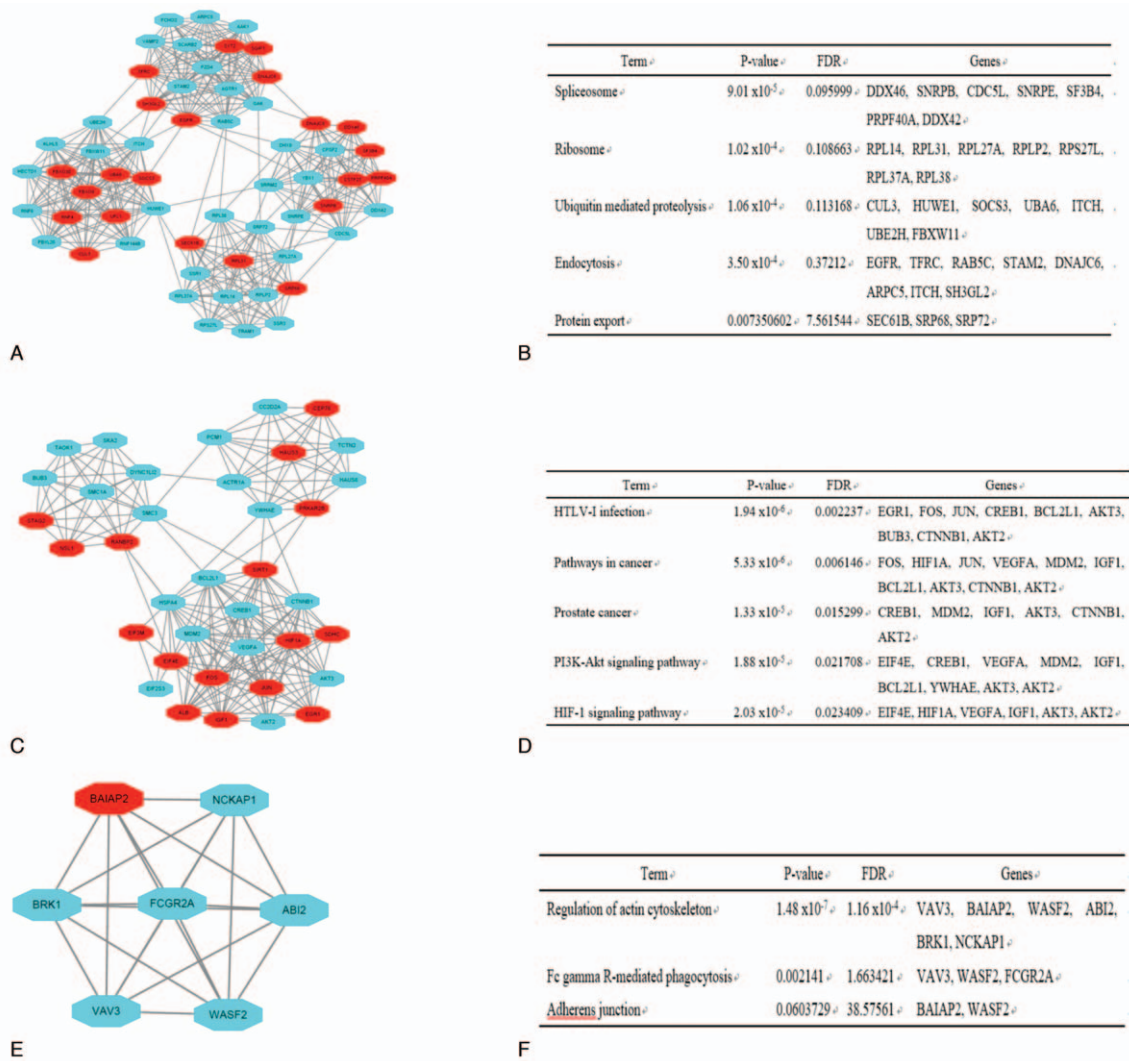


Figure 2. Top 3 modules from the protein-protein interaction network. (A) module 1, (B) the enriched pathways of module 1, (C) module 2, (D) the enriched pathways of module 2, (E) module 3, (F) the enriched pathways of module 3.

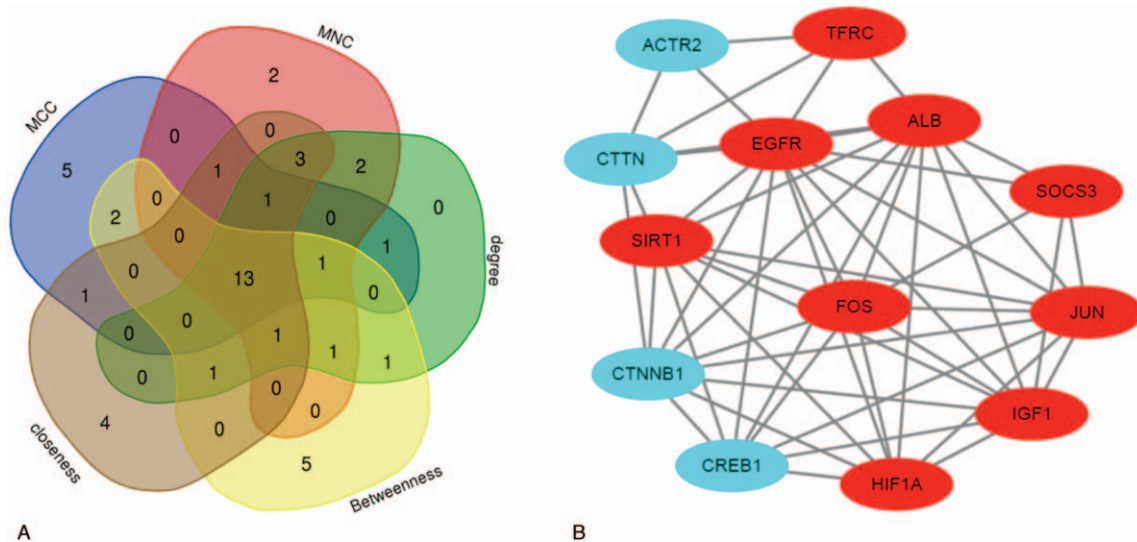


Figure 3. (A) Overlapping DEGs among cytoHubba of the 5 methods; (B) PPI network of the 13 hub genes. DEGs = differentially expressed genes.

Table 4
The information of 13 hub genes.

Gene	MCC	MNC	Degree	Closeness	Betweenness
FOS	7495133	52	55	287.2333	13714.02
EGFR	7686237	74	83	324.9167	67299.81
SIRT1	7306829	48	51	287.9333	18851.81
ALB	7329846	66	70	311.3333	45462.88
TFRC	363847	27	28	263.1	7988.437
JUN	7454347	59	60	298.4833	21627.76
IGF1	3694077	46	49	288.8667	14570.83
HIF1A	7263218	22	26	271.95	8651.352
SOCS3	369166	27	29	263.65	8000.68
ACTR2	363101	30	31	259.8167	8919.981
CREB1	7407142	44	48	287.0833	17167.61
CTNNB1	7325482	57	61	299.7167	26334.02
CTTN	363962	28	30	273.15	10175.78

organ systems.^[25] In the early stages of IgAN, the VEGF expression increases at least in part by local tissue hypoxia through an HIF-1 α -relying pathway to maintain the number of PTC, but this salvage mechanism in reaction to tissue hypoxia fails in the advanced stages.^[26] MiR-29c can be down-regulated by renal interstitial fibrosis in IgAN, and up-regulated by HIF-1 α activation to alleviate fibrosis.^[27]

The new soluble transferrin receptor (TfR or CD71) of IgA1 is expressed on mesangial cells.^[28] IgA precipitation is connected with higher expression of CD71 and is first linked with CD71 expression. Double-labeled research with confocal microscopy shows that the IgA deposits mostly localize together with CD71 mesangially.^[29] CD71 is probably the main receptor that mediates mesangial IgA precipitation and the IgA and CD71 interaction and the consequences on mesangial cells may explain the pathogenesis of IgAN.

In conclusion, some key genes closely related with the bioprocesses and signaling pathways in IgAN initiation and progression were screened out. We identified 9 novel genes that were not reported before and may be imperative in IgAN. These genes can be potentially used to molecularly diagnose or cure IgAN. Nevertheless, further research is needed to explore the mechanisms of these genes in IgAN.

Author contributions

Conceptualization: Shou-Liang Hu.

Methodology: Fan-Li Yuan.

Supervision: Qing-Feng Lei.

Visualization: Dan Wang.

Writing – original draft: Shou-Liang Hu, Dan Wang.

Writing – review & editing: Jun-Zhang Cheng.

References

- Berger J, Hinglais N. Intercapillary deposits of IgA-IgG. *J Urol Nephrol* (Paris) 1968;74:694–5.
- D'Amico G. The commonest glomerulonephritis in the world: IgA nephropathy. *Q J Med* 1987;709:709–27.
- McGrogan A, Franssen CF, de Vries CS. The incidence of primary glomerulonephritis worldwide: a systematic review of the literature. *Nephrol Dial Transplant* 2011;26:414–30.
- O'Shaughnessy M, Hogan S, Bawana D, et al. Glomerular disease frequencies by race, sex, and region: from the International Kidney Biopsy Survey (IKBS). *Nephrol Dial Transplant* 2018;33:661–9.
- D'Amico G. Natural history of idiopathic IgA nephropathy and factors predictive of disease outcome. *Semin Nephrol* 2004;24:179–96.

- Durchdewald M, Angel P, Hess J. The transcription factor Fos: a Janus-type regulator in health and disease. *Histol Histopathol* 2009;24:1451–61.
- Takemura T, Okada M, Akano N, et al. Proto-oncogene expression in human glomerular diseases. *J Pathol* 1996;178:343–51.
- Rastaldi MP, Tunesi S, Ferrario F, et al. Transforming growth factor-beta, endothelin-1, and c-fos expression in necrotizing/crescentic IgA glomerulonephritis. *Nephrol Dial Transplant* 1998;13:1668–74.
- Ebihara I, Nakamura T, Suzuki S, et al. Protooncogene expression in peripheral blood mononuclear cells in IgA nephropathy. *Kidney Int* 1991;39:946–53.
- Park HJ, Kim JW, Cho BS, et al. Association of FOS-like antigen 1 promoter polymorphism with podocyte foot process effacement in immunoglobulin A nephropathy patients. *J Clin Lab Anal* 2014;28:391–7.
- Jiang H, Liang L, Qin J, et al. Functional networks of aging markers in the glomeruli of, IgA nephropathy: a new therapeutic opportunity. *Oncotarget* 2016;7:33616–26.
- Rabkin R, Schaefer F. New concepts: growth hormone, insulin-like growth factor-I and the kidney. *Growth Horm IGF Res* 2014;24:270–6.
- Alric C, Pecher C, Cellier E, et al. Inhibition of IGF-1-induced Erk 1 and 2 activation and mitogenesis in mesangial cells by bradykinin. *Kidney Int* 2002;62:412–21.
- Tack I, Elliot SJ, Potier M, et al. Autocrine activation of the IGF-I signaling pathway in mesangial cells isolated from diabetic NOD mice. *Diabetes* 2002;51:182–8.
- Isshiki K, He Z, Maeno Y, et al. Insulin regulates SOCS2 expression and the mitogenic effect of IGF-1 in mesangial cells. *Kidney Int* 2008;74:1434–43.
- Hahn WH, Suh JS, Cho BS. Polymorphisms of insulin-like growth factor-1 (IGF-1) and IGF-1 receptor (IGF-1R) contribute to pathologic progression in childhood IgA nephropathy. *Growth Factors* 2011;29:8–13.
- Wei L, Fu R, Liu X, et al. Rs1520220 and Rs2195239 polymorphisms of IGF-1 gene associated with histopathological grades in IgA nephropathy in Northwestern Chinese Han population. *Kidney Blood Press Res* 2018;43:80–7.
- Conde E, Alegre L, Blanco-Sánchez I, et al. Hypoxia inducible factor 1-alpha (HIF-1alpha) is induced during reperfusion after renal ischemia and is critical for proximal tubule cell survival. *PLoS One* 2012;7:e33258.
- Kojima I, Tanaka T, Inagi R, et al. Protective role of hypoxia-inducible factor-2a against ischemic damage and oxidative stress in the kidney. *J Am Soc Nephrol* 2007;18:1218–26.
- Zhang L1, Huang H, Cheng J, et al. Pre-treatment with isoflurane ameliorates renal ischemic-reperfusion injury in mice. *Life Sci* 2011;88:1102–7.
- Higgins DF, Johnson RS, Haase VH. Hypoxic signaling enhances renal fibrosis (Hypoxia and Development, Physiology and Disease, Breckenridge, CO, Keystone Symposia), Silverthorne, CO: Keystone Symposia on Molecular and Cellular Biology; 2006:74.
- Kimura K, Iwano M, Akai Y, et al. HIF-1 α is a key molecule for the progression of EMT-mediated renal fibrosis. *ASN Annual Meeting, Philadelphia, PA* (Abstract). *J Am Soc Nephrol* 2005;16:656A.
- Manotham K, Tanaka T, Matsumoto M, et al. Transdifferentiation of cultured tubular cells induced by hypoxia. *Kidney Int* 2004;65:871–80.
- Bohle A, Mackensen-Haen S, Wehrmann M. Significance of post-glomerular capillaries in the pathogenesis of chronic renal failure. *Kidney Blood Press Res* 1996;19:191–5.
- Ferrara N, Davis-Smyth T. The biology of vascular endothelial growth factor. *Endocr Rev* 1997;18:4–25.
- Namikoshi T, Satoh M, Horike H, et al. Implication of peritubular capillary loss and altered expression of vascular endothelial growth factor in IgA nephropathy. *Nephron Physiol* 2006;102:9–16.
- Fang Y, Yu X, Liu Y, et al. miR-29c is downregulated in renal interstitial fibrosis in humans and rats and restored by HIF-1 α activation. *Am J Physiol Renal Physiol* 2013;304:F1274–82.
- Moura IC, Centelles MN, Arcos-Fajardo M, et al. Identification of the transferrin receptor as a novel immunoglobulin (Ig)A1 receptor and its enhanced expression on mesangial cells in IgA nephropathy. *J Exp Med* 2001;194:417–25.
- Haddad E, Moura IC, Arcos-Fajardo M, et al. Enhanced expression of the CD71 mesangial IgA1 receptor in Berger disease and Henoch-Schönlein nephritis: association between CD71 expression and IgA deposits. *J Am Soc Nephrol* 2003;14:327–37.